CHEMICAL ENGINEERING TRANSACTIONS
VOL. 92, 2022
A publication of AIDIC
The Italian Association of Chemical Engineering
Online at www.cetjournal.it
Guest Editors: Rubens Maciel Filho, Eliseo Ranzi, Leonardo Tognotti

ISBN 978-88-95608-90-7; **ISSN** 2283-9216
DOI: 10.3303/CET2292007

Effects of Ni-Co Ratio on Deactivation and Coke Formation in Steam Reforming of Hydrocarbon Impurities from Biomass Gasification with Ni-Co/Mg(Al)O Catalysts

Ask Lysne, Kristin Ø. Madsen, Jibin Antony, Kumar R. Rout, Edd A. Blekkan*

Department of Chemical Engineering, Norwegian University of Science and Technology
edd.a.blekkan@ntnu.no

Ni-Co/Mg(Al)O catalysts with different Ni-Co ratios (40-0, 30-10, 20-20, 10-30 and 0-40 wt%) have been tested for steam reforming of hydrocarbon impurities in a model biomass gasification syngas at relevant operating conditions. Effects of tar model (toluene) presence on catalyst deactivation and coke formation were studied. The fresh samples were characterized by ICP-MS, XRD, TPR, N_2-physisorption and H_2-chemisorption. The coke formation was studied by TGA-TPO, Raman spectroscopy and SEM/EDS. Efficient formation of Ni-Co alloy particles was confirmed by XRD and SEM/EDS. The Ni-Co/Mg(Al)O system shows high steam reforming activity with complete model tar removal. Simultaneous high-temperature H_2/CO ratio adjustment by effective equilibration of the WGS reaction was demonstrated. Initial Co addition was proposed to reduce the formation of strongly deactivating encapsulating coke species by efficient removal of coke precursors at the expense of enhanced carbon filament formation. Lower Ni-Co ratios were shown to effectively reduce deactivation and coke formation at the expense of the higher initial activity of the high Ni-Co ratio system. Restructuring of extensive carbon filament clusters was proposed as an additional route to encapsulating coke species with potential long-term deactivation effects. The Ni-Co ratio was shown to affect the carbon filament formation rates and filament diameter distributions. The effects on coke formation were proposed to depend on complex interactions of metal particle size and Ni-Co alloy ratio. The results contribute to the understanding of the highly attractive resistance towards deactivation by coke formation of Ni-Co catalyst systems.

1. Introduction

Renewable aviation fuels can be produced in a biomass-to-liquid process, coupling biomass gasification and Fischer-Tropsch synthesis (Huber et al., 2006). Biomass gasification involves thermal decomposition of biomass feedstocks, forming mainly H_2, CO, CO_2, CH_4 and H_2O (Giuliano et al., 2020). The product gas also contains tar impurities (condensable aromatic hydrocarbons) causing downstream condensation, coking and corrosion issues (Li et al., 2015). Tar elimination has been put forth as the greatest challenge in commercialization of such technologies. Steam reforming is an attractive tar removal approach, increasing process efficiency compared to physical separation and thermal cracking strategies. Li et al. (2015) reviewed the development of catalysts for such applications, calling for further research on bi-metallic Ni-Co systems, targeting low-cost, high-performance alloy catalysts with increased coke formation resistance. Hydrotalcite-based Ni-Co/Mg(Al)O catalysts have to the best of our knowledge never been reported for tar removal at relevant operating conditions. The goal of the present work was to study the effects of Ni-Co ratio on reforming activity and stability of such systems. The coke characterization approach provides further understanding of coke formation dynamics in Ni-Co catalysts.

2. Experimental

The catalyst synthesis was based on previous literature (He et al., 2009). All chemicals were acquired from Sigma-Aldrich or VWR Chemicals. Reduced and passivated samples were prepared by reduction at 670 °C for 16 hours in H_2 (200 NmL/min) and He (100 NmL/min). The samples were cooled in He (100 NmL/min) and passivation in 1 mol% O_2 in N_2 (100 NmL/min) for 2 hours.

Paper Received: 11 February 2022; Revised: 12 March 2022; Accepted: 5 May 2022
Please cite this article as: Lysne A., Madsen K.O., Antony J., Rout K.R., Blekkan E.A., 2022, Effects of Ni-Co Ratio on Deactivation and Coke Formation in Steam Reforming of Hydrocarbon Impurities from Biomass Gasification with Ni-Co/Mg(Al)O Catalysts, Chemical Engineering Transactions, 92, 37-42 DOI:10.3303/CET2292007

2.1 Catalyst characterization

ICP-MS was performed by SINTEF. The calcined precursors were decomposed in parallel with HCl and HNO_3 at 250 °C for 10 minutes in a Milestone UltraWAVE microwave oven and analyzed with an Agilent 8800 Triple Quadrupole ICP-MS equipped with an SPS 4 Autosampler. The samples were diluted in 5% HNO_3 and added ^{115}In as internal standard. Quantification was performed with respect to standards from Inorganic Ventures. Powder XRD was conducted with a Bruker D8 A25 DaVinci X-ray Diffractometer. TPR was performed with an Altamira BenchCat Hybrid 1000HP. The samples were pre-dried at 200 °C for 30 minutes in Ar (50 NmL/min) and cooled to 50 °C before heating to 900-1000 °C in 7 mol% H_2 in Ar (50 NmL/min). N_2-physisorption was carried out with a Micromeritics TriStar 3000 Surface Area and Porosity Analyzer. The samples (280 mg) were degassed in vacuum for 1 hour at room temperature and overnight at 100 °C. Adsorption/desorption isotherms were recorded at -196 °C. H_2-chemisorption was performed with a Micrometrics ASAP 2020 instrument. The calcined samples (150 mg) were evacuated for 1 hour at 30 °C and reduced in H_2 at 670 °C for 16 hours. The system was evacuated for 0.5 hours at 670 °C and 1.5 hours at 35 °C before recording the adsorption isotherms.

2.2 Steam reforming experiments

The experimental setup is shown in Figure 1. Reforming experiments were performed with a fixed-bed quartz reactor (6 mm inner diameter) with catalyst samples (10.0 mg, 75-150 µm) diluted with α-Al_2O_3 (400.0 mg). Reaction temperatures were measured with a thermocouple in a reactor center heat-pocket in contact with the top of the catalyst bed. All gasses were fed by Bronkhorst MFCs. The model syngas contained 10/35/25/25 mol% $CH_4/H_2/CO/CO_2$ with 5 mol% N_2 as internal standard. The steam was provided with a vaporizer consisting of an MFC feeding H_2O through a heating furnace (250 °C, Ar carrier gas) from a pressurized water-tank. All lines downstream of the vaporizer were heated to avoid condensation. The catalysts were reduced in 50 mol% H_2 (100 NmL/min) in Ar (100 NmL/min) for 16 hours at 670 °C. The reactant flow was stabilized in a reactor bypass before directing the flow to the catalyst. The syngas flow (400 NmL/min), GHSV (85000 NmL/g_{cat}min), pressure (atmospheric) and S/C ratio of 3.0 (molar hydrocarbon basis) were kept constants for all experiments.

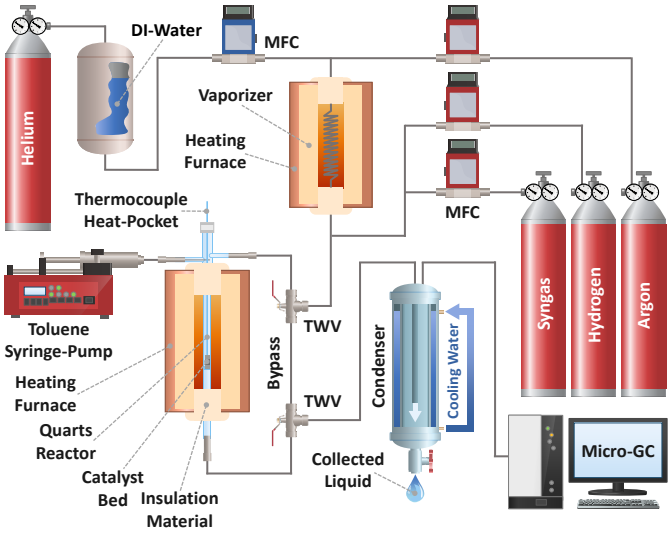

Figure 1: Simplified experimental setup. Syngas: 400 NmL/min, toluene: 10.0 g/Nm^3 (dry syngas basis), GHSV: 85000 NmL/g_{cat}min, temperature: 650-800 °C, S/C ratio: 3.0 (molar hydrocarbon basis).

Initial empty-reactor tests were performed at the same conditions. Initial SMR temperature screening was carried out at 650-800 °C. The catalyst stability during SMR operation was studied for 8 hours at 700 °C. The stability during hydrocarbon steam reforming in a tar model environment was studied by injection of 10.0 g/Nm^3 toluene (dry syngas basis) into the reactor with an NE-1000 syringe-pump (50 mL SS syringe, KD Scientific). Condensable liquids were removed before gas composition analysis (CH_4, H_2, CO, CO_2 and N_2) with an Agilent 490 Micro-GC system (CP-COX column). Spent catalysts were cooled to room temperature in Ar (100 NmL/min) and isolated from the dilution material by magnetic separation. Condenser samples were extracted (n-pentane) and analyzed with an Agilent 7820A GC-FID system (HP-5 column). Peak identification was achieved with an Agilent 7820A GC-MS system. All applied gases were supplied by Linde/AGA. Equilibrium compositions were calculated in Aspen Plus V9 (Peng-Robinson cubic equation of state).

2.3 Coke characterization

TGA-TPO was performed with an Linseis STA PT1600 instrument, heating the spent catalysts (5-10 mg) from 150 to 800 °C (5 °C/min) in synthetic air (21 mol% O_2 in N_2, 140 NmL/min) and Ar (60 NmL/min) after 1 hour of pre-drying at 150 °C in Ar (200 NmL/min). The coke combustion was monitored by CO_2 formation with an MS detector (m/z = 44). Raman spectroscopy was carried out with a Horiba Jobin Yvon LabRAM HR800 system (633 nm laser). SEM/EDS was performed with an ultra-high resolution Hitachi SU9000 STEM instrument. The spent samples were dispersed in ethanol and drop-casted onto plasma cleaned diced silicon wafers. Elemental mapping was performed with an Oxford Ultim Extreme EDS detector.

3. Results and discussion

Initial empty-reactor tests showed negligible SMR and WGS activity within the inaccuracy of the measurements. Ideal plug-flow conditions and elimination of mass-transfer limitations were acquired by preliminary calculations recommended by the EUROKIN project. Initial temperature screening gave linear Arrhenius plots at lower temperatures (650-700 °C) as expected in the kinetic regime. Further tests were conducted at 700 °C to study deactivation of intrinsic kinetics. The CH_4 conversion was far from thermodynamic equilibrium in all experiments. The carbon mass balance was 99.0±0.9% for all data, indicating high quality feed and product analysis control.

3.1 Catalyst characterization

XRD and TPR results were in accordance with previously reported data (He et al., 2009). Key ICP-MS data is shown in Table 1. The bulk Ni/Co ratios were generally slightly higher than target values. This was in accordance with previous literature relating the effect to restricted integration of Co into the hydrotalcite structure (compared to Ni) due to the larger atomic radius (He et al., 2009).

Table 1: Key ICP-MS data (average from two samples).

Sample	Ni (%)	Co (%)	Mg (%)	Al (%)	Ni/Co ratio (a.u.)
40 wt% Ni	35.5	-	38.5	26.0	-
30-10 wt% Ni-Co	27.4	8.9	36.1	27.6	3.08
20-20 wt% Ni-Co	18.4	17.6	37.0	27.0	1.05
10-30 wt% Ni-Co	9.5	26.2	36.2	28.1	0.36
40 wt% Co	-	34.8	38.7	26.5	-

XRD patterns after reduction and passivation (Figure 2a) showed complete reduction of spinel-type structures leaving only the MgO-like support and metallic Ni and Co. Figure 2b shows an observed shift in d-spacing towards higher values with increasing Co content due to the larger atomic radius.

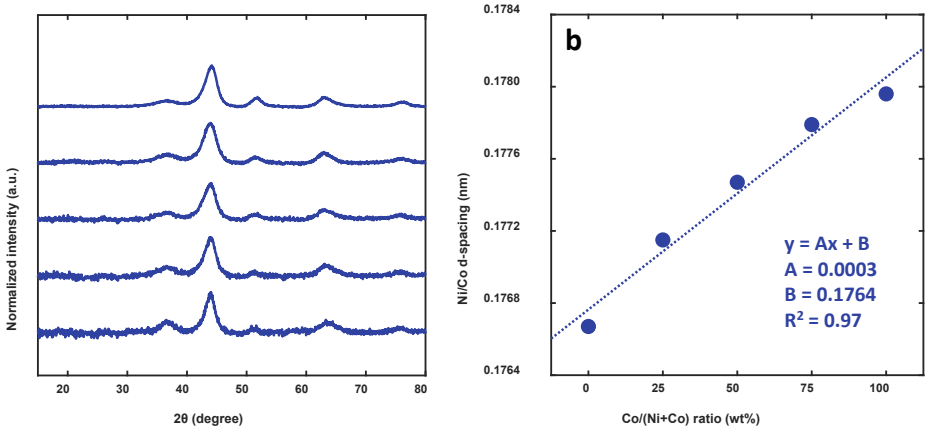

Figure 2: XRD patterns (a) after reduction and passivation with MgO-like mixed oxide supports (◈) and metallic Ni-Co particles (◆). (b) Shifted Ni-Co crystal plane d-spacing.

The close to linear relation suggested effective formation of Ni-Co alloy particles. Efficient Ni-Co alloy formation was confirmed by SEM/EDS elemental mapping showing clear co-location of Ni/Co in metal particles. EDS point scans (20 particles) gave Ni/Co ratios of 4.3±0.5, 1.1±0.1 and 0.42±0.04 for the 30-10, 20-20 and 10-30 wt%

Ni-Co samples, somewhat higher than ICP-MS bulk ratios. Key N_2-physisorption and H_2-chemisorption data is shown in Table 2. The highest BET surface areas and metal dispersions were obtained at higher Ni-Co ratios.

Table 2: Key N_2-physisorption (average from two samples) and H_2-chemisorption data.

Sample	BET surface area (m^2/g)	Metal dispersion (%)	Metal particle diameter (nm)
40 wt% Ni	175	8.1	12.6
30-10 wt% Ni-Co	184	8.6	11.8
20-20 wt% Ni-Co	162	6.5	15.4
10-30 wt% Ni-Co	151	4.8	20.7
40 wt% Co	118	5.4	18.5

3.2 Catalyst deactivation

Catalyst reforming activity was monitored by CH_4 conversion with and without tar model (toluene) presence. Typical conversion profiles are shown in Figure 3a with simple linear decay functions in the pure syngas. Tar model presence gave initial rapid exponential deactivation followed by further linear decay. An expected toluene addition delay (20-30 min) from the tubing between the syringe-pump and the reactor was observed. No toluene or other byproducts were found in the condenser samples. Standard analysis indicated toluene conversions well above 99.5% (equilibrium = 100%). Initial and final (TOS = 8 hours) CH_4 conversions are shown in Figure 3b.

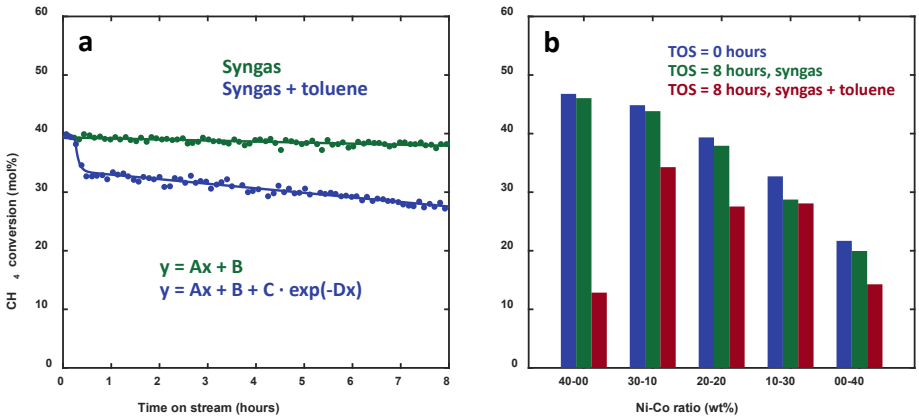

Figure 3: CH_4 conversion profiles (a) in pure syngas and tar model (toluene) environment (20-20 wt% Ni-Co). (b) Initial and final (TOS = 8 hours) CH_4 conversion with different Ni-Co ratios.

The reforming activity was fairly stable for all samples in the pure syngas. Interestingly, the 30-10 wt% Ni-Co and 40 wt% Ni samples showed similar high initial activities, but with considerably reduced deactivation in the bi-metallic system. Figure 3b shows how the final reforming activity of the lower Ni-Co ratio samples is limited by the decreasing initial activity upon Co addition. Similar effluent H_2/CO ratios (1.77-1.91) were obtained for all samples throughout the experiments despite the changing CH_4 conversion. Such behavior is expected in the case of effective equilibration of the WGS reaction. The H_2/CO ratios were close to calculated equilibrium values (1.65-1.75). Only the highly deactivated 40 wt% Ni sample showed some WGS activity loss by a small H_2/CO ratio decrease (final value of 1.57) in the tar model environment.

3.3 Coke characterization

Figure 4a shows coke amounts and combustion CO_2 signals from TGA-TPO after operation in the tar model environment. The Raman spectra for the same samples are shown in Figure 4b. Interestingly, the highest coke amount was found for the 30-10 wt% Ni-Co sample. Such high coke amounts despite a lower overall deactivation can be explained by carbon filament formation without active site blockage. Chen et al. (2005) studied filament growth in Ni catalysts, observing rapid deactivation of smaller metal particle samples. The present work similarly shows rapid deactivation of the 40 wt% Ni catalyst with small metal particles (12.6 nm). The deactivation of smaller particles was explained by a reduced carbon diffusion driving force (bulk diffusion model) increasing carbon surface coverage, carbon polymerization rates and the formation of strongly deactivating encapsulating coke (Chen et al., 2005). This model was in accordance with the high-temperature coke combustion shift observed for the 40 wt% Ni sample. Higher temperature coke combustion is generally associated with a higher

degree of encapsulation since available active metal sites also catalyze combustion reactions. These results suggest that the 30-10 wt% Ni-Co sample forms less encapsulating coke compared to the 40 wt% Ni catalyst. The effect is however proposed to result from effective removal of coke precursors from the particle surface at the expense of enhanced filament growth. The altered coke formation for the two catalysts with similar metal particle size (11.8-12.6 nm), suggested some additional Ni-Co synergy effects beyond metal particle size alone. The lower coke amounts upon further Co addition indicated reduced filament growth despite the metal particle size increase (15.4-20.7 nm). The Raman spectra showed the expected D and G bands (1350 and 1580 cm^{-1}) attributed to the presence of disordered/defective carbon and ordered graphitic structures respectively. No detectable coke was found by TGA-TPO or Raman spectroscopy for any samples after tar free operation.

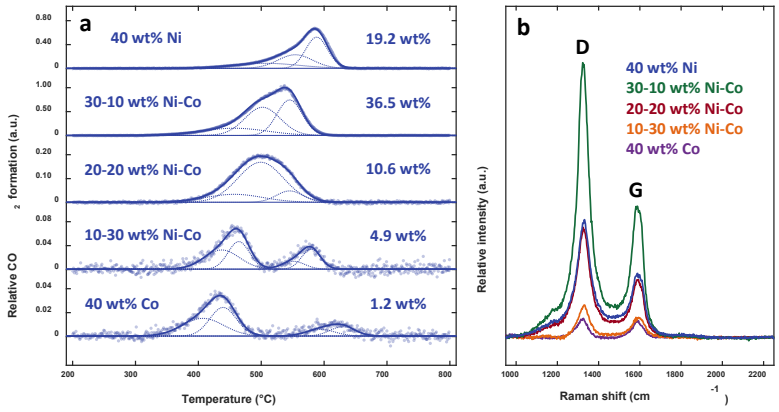

Figure 4: (a) CO_2 formation (coke combustion) during TGA-TPO after operation in tar model (toluene) presence (note individual y-axis scaling). Estimated coke amounts indicated. (b) Raman spectra for the same samples.

Figure 5a shows regions with encapsulating coke particularly prominent in the 40 wt% Ni sample. Figure 5b shows regions with less encapsulation frequently observed at lower Ni-Co ratios. This suggested the highly encapsulating coke species to be less developed in these samples in accordance with TGA-TPO results. Figure 5c shows carbon filament clusters found in all samples, confirming the previous indications of filament formation. Figure 5d shows what appeared to be fused filament clusters. Such filament aging is described in previous literature with potential long-term blocking of catalyst pores and metal sites (Montero et al., 2015). Figure 5e shows normalized filament diameter distributions (1000 filaments). Interestingly, the 30-10 and 20-20 wt% Ni-Co showed shifted filament distributions towards larger diameters (10-60 nm). These samples also showed considerably higher linear decay components (A = 0.0130 and 0.0134) in the tar model environment compared to the other catalysts (A = 0.0015 to 0.0057). It is reasonable to believe that the broader filament diameter selectivity can be related to enhanced filament growth and the TGA-TPO peaks around 500 °C with the highest intensities in the same samples. The higher linear decay is proposed to result from filament restructuring mechanisms. Further Co addition limits filament formation to smaller diameters (5-35 nm). It is reasonable to believe that the lower coke amounts at low Ni-Co ratios can be related to a reduced filament growth following the shifted diameter selectivity. The filament diameter is generally considered to reflect the size of the metal particle from which the filament grows. Figure 5e shows the metal particle size distribution (1000 particles) for the 20-20 wt% Ni-Co sample, with the filament distribution covering the lower particle size range. The selectivity towards smaller particles with higher surface area and density of steps is not unexpected. In a bulk diffusion model the shorter diffusion length and higher diffusion flux area of smaller particles is also expected to enhance filament growth. However, Chen et al. (2005) showed that smaller particles give higher filament saturation concentrations, reducing the bulk diffusion driving force. The net particle size effect on filament growth rates will depend on the compensation of these factors. The enhanced filament formation in the 30-10 wt% Ni-Co sample compared to the 40 wt% Ni catalyst with similar metal particle size suggests the net particle size effect to be altered upon Co addition. Steady-state filament growth rates are commonly considered to reflect carbon bulk diffusion rates. The lower carbon diffusion coefficient in Co ($8.17 \cdot 10^{-14}$ m^2/s) compared to Ni ($3.03 \cdot 10^{-13}$ m^2/s) at 700 °C (Yokoyama et al., 1998) could hereby explain the reduced filament formation at lower Ni-Co ratios. The low formation of encapsulating coke in these samples can be explained by enhanced coke gasification, or simply by lower carbon surface concentrations due to the lower reforming activity.

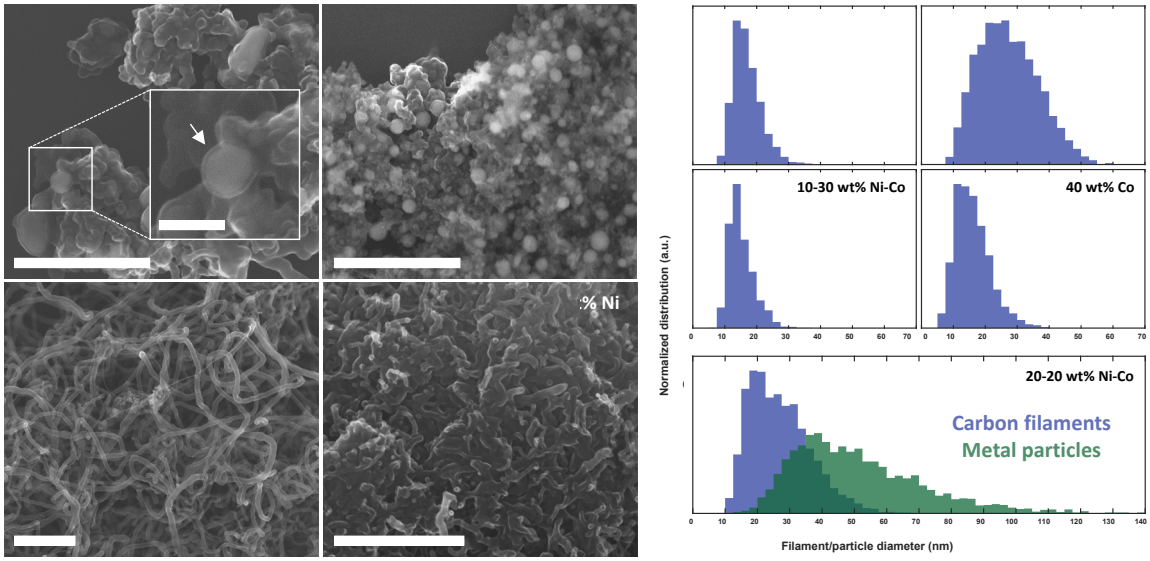

Figure 5: SEM images of (a) encapsulating coke, (b) less encapsulated regions, (c) carbon filament clusters and (d) fused filaments. (e) Normalized filament/metal particle diameter distributions.

4. Conclusions

The Co addition effectively reduced the formation of strongly deactivating encapsulating coke species compared to the mono-metallic Ni catalyst. The effect was attributed to efficient removal of surface carbon at the expense of enhanced carbon filament formation. The performance of low Ni-Co ratio catalysts was limited by the lower initial reforming activity. Filament growth and diameter selectivities were proposed to depend on complex metal particle size and Ni-Co ratio interactions. These results contribute to the understanding of the highly attractive resistance towards deactivation by coke formation of Ni-Co reforming catalysts.

Acknowledgments

The project is funded by the Norwegian Research Council (no. 257622) through the Centre for Environment-friendly Energy Research (FME) Bio4Fuels. The Norwegian Research Council is also acknowledged for the support to the Norwegian Micro- and Nano-Fabrication Facility, NorFab (no. 295864).

References

Chen D., Christensen K.O., Ochoa-Fernández E., Yu Z., Tøtdal B., Latorre N., Monzón A., Holmen A., 2005, Synthesis of carbon nanofibers: effects of Ni crystal size during methane decomposition, Journal of Catalysis, 229, 82-96.

Giuliano A., Freda C., Catizzone, E., 2020, Techno-Economic Assessment of Bio-Syngas Production for Methanol Synthesis: A Focus on the Water-Gas Shift and Carbon Capture Sections, Bioengineering, 7, 70.

He L., Berntsen H., Ochoa-Fernández E., Walmsley J.C., Blekkan E.A., Chen D., 2009, Co-Ni Catalysts Derived from Hydrotalcite-Like Materials for Hydrogen Production by Ethanol Steam Reforming, Topics in Catalysis, 52, 206-217.

Huber G.W., Iborra S., Corma A., 2006, Synthesis of Transportation Fuels from Biomass: Chemistry, Catalysts, and Engineering, Chemical Reviews, 106, 4044-4098.

Li D., Tamura M., Nakagawa Y., Tomishige K., 2015, Metal catalysts for steam reforming of tar derived from the gasification of lignocellulosic biomass, Bioresource Technology, 178, 53-64.

Montero C., Ochoa A., Castaño P., Bilbao J., Gayubo A.G., 2015, Monitoring Ni^0 and coke evolution during the deactivation of a Ni/La_2O_3-αAl_2O_3 catalyst in ethanol steam reforming in a fluidized bed, Journal of Catalysis, 331, 181-192.

Yokoyama H., Numakura H., Koiwa M., 1998, The Solubility and Diffusion of Carbon in Palladium, Acta Materialia, 46, 2823-2830.